

## Sequencing & design of processing instruments alter the degree of dispersion of clays and mechanical properties of nanocomposites

Balwinder Ghuman<sup>1</sup>

<sup>1</sup>Dr Shanti Swaroop Bhatnagar University Institute of Chemical Engineering & Technology, Panjab University, Sector-14, Chandigarh, India-160014 (formerly Department of Chemical Engineering & Technology)  
[balwinderghuman@hotmail.com](mailto:balwinderghuman@hotmail.com)

### Abstract

Polyurethane coatings reinforced with nano clay especially organo-modified clay, show high sensitivity to changes in structure, properties, and performance when the sequence and design of its processing instruments are slightly altered. Using 1 weight percentage cloisite C30B nano-filled polyurethane coating formulations, we demonstrate that a combination of probe sonicator (PS) and ultrasonic bath (USB) can process these coatings into structurally different nanocomposite coatings possessing varied properties. In process-P, we combined the PS and USB into parallel (simultaneous usage) while in process-S we used USB first and PS later for processing the

2nd October, 2021

formulations in series combinations. These coating formulations were characterized for mechanical and barrier properties and tried to correlate with the degree of dispersion of clays in the PU matrix. The effect of the design of processing instruments on mechanical properties was studied by replacing PS with M (Mechanical homogenizing mixer) in parallel and series sequencing. This kind of sensitivity to processing sequences for these nanocomposite coatings was unknown and requires greater investigations for generalizing the results for all other nanofillers.

**Keywords:** Polyurethanes (PU), Cloisite C30B, Probe sonicator (PS), Ultrasonic bath (USB), Mechanical homogenizing mixer (M), Nano-filler, Nano-composites

## Introduction

Coatings provide a protective layer over the substrate surface, giving the substrate a decorative look, covering them from external environmental threats, act as an impressive barrier, for retarding the penetration of moisture, corrosive chloride ions, acids, and biological attacks [1]. Polyurethane (PU) coatings are assumed to be tough, have good

strength and a high pitch on clarity, excellent adhesion properties, hydrophobic, high gloss, good mechanical properties, excellent flexibility, elastic recovery, and good chemical resistance [1,2]. Acrylic polyols and an aliphatic ring of diisocyanate give tough, more light stable, and transparent coatings [3-5]. PU is the most popular material in the polymer industry and is widely used especially in motor vehicles, furniture coatings, synthetic resins, synthetic leather, construction materials, paints and elastomers, sealants, foams, and fibers [2,6].

PUs are block copolymers that contain hard and soft segments, semi-crystalline hard segments which are formed by the reaction of chain extenders and isocyanates whereas amorphous soft segments consist of long-chain polyols [2]. The raw materials used, their molecular structure, composition, processing techniques govern the properties of PUs, which can be tailored to produce a broad range of applications. However, the inferior gas barrier properties of PUs put some restrictions on exploring the use and applications of various challenging fields. The thermodynamic immiscibility of two segments (Soft segment and hard segment) that results in phase separation of the

microstructure is the main reason behind the inferior gas barrier properties [2].

PUs contain urethane as a main repeating unit [6]. The properties of PUs can be tailored in two ways 1) by changing the chemistry of PUs by changing the molecular structure of raw materials i.e. soft segment and hard segment 2) adding nanofillers to the PUs such as calcium carbonate, aluminum hydroxide,  $\text{TiO}_2$ ,  $\text{ZnO}$ , silica [2,6,7]. Nanofillers like  $\text{ZnO}$ ,  $\text{TiO}_2$ ,  $\text{SiO}_2$  [8-10], and various clays with different modifiers have been explored.

The conventionally added fillers to PU coatings improve the mechanical properties, scratch-wear resistance, pigmentation and impart more thermal and UV stability but diminish gloss, clarity, and transparency [11-15]. The fillers are explored on the nano-scale nowadays to exploit the properties like gloss, clarity, and transparency. Cloisites below 500nm dimensions may not impart any color [16]. The particle size of the nanofillers affects the performance of the coatings and a critical particle size exists for a particular system of nanofiller and matrix where maximum particular properties can be achieved [9]. Clays are having a capacity to exhibit an excellent choice to work as a

nanofiller due to its properties like low density, abundant availability, low cost, large specific surface area, high aspect ratio, economic competitiveness, and high strength of clay particles [2,6,14]. The best performance of nano-composites is achieved when clay silicate layers have a maximum degree of interaction with the PU matrix, and are fully exfoliated and well dispersed in the PU matrix, moreover hybrid nanostructures are obtained with intercalated to exfoliated structures [7]. There are number of clay minerals, but clays used for polymer nano-composites belong to phyllosilicates. The 2:1 phyllosilicate consists of one octahedral sheet of alumina or magnesium are sandwiched between two tetrahedral sheets of silica(Si-O). The interlayer gallery spacing is occupied by exchangeable inorganic cations such as  $\text{Ca}^{+2}$ ,  $\text{Na}^+$ , etc., and moisture. Pristine clay platelets are not compatible with most of the polymeric systems due to their hydrophilic nature. However, the cation exchange process of clay platelets with alkyl ammonium or alkyl phosphonium quaternary ions enhance the clay polymer interactions and dispersion of clay platelets into the polymer matrix. Cation modifications are required to increase the gallery spacing or d-

spacing between the silicate layers to allow the high incorporation of polymer chains. The clay/polymer compatibility, as well as exfoliation of clay silicates layers, depends upon the type of modifier and polarity of the system [2,6,7,17].

Cloisite C30B is swellable montmorillonite [7], belongs to the smectite group, the clay having the general formula  $(\text{Na,Ca})_{0.33}(\text{Al,Mg})_3(\text{Si}_4\text{O}_{10})(\text{OH})_2.n\text{H}_2\text{O}$  with an interlayer spacing of 1.2nm [2,7,18]. C30B contains –OH group present in its modifier and thus exhibits better dispersion into the polymer matrix, shows good strength, stiffness, and flame retarding properties. Cloisite C30B is used for reinforcement properties, heat distortion properties, thermal expansion, and barrier properties. Cloisite C30B is modified by methyl tallow bis-2-hydroxyethyl quaternary ammonium (MT2EOH) and contains one tallow group in its organic modifier, which hardly shields the surface of silicate platelets from polymer, also do not prevents polymer chains to penetrate the gallery spacing. Cloisite C30B also contains two –OH groups present in its organic modifier and makes good interactions with the polymer system due to hydrogen bonding, which may result in a higher degree of exfoliation and a

high increase in d-spacing [19]. The nano-clay platelets have the potential to increase the mechanical properties of the PU when properly dispersed, exfoliated, and oriented in the polymer matrix. The mechanical properties can be improved by the nano-platelets because of the reason a) clays make hydrogen/covalent bonding between hardener of PU and modifier of clays b) by increasing the interfacial interactions between nano-platelets and the polymer matrix by cross-linking.

To achieve the optimal properties of PU/clay nano-composites and also to take advantage of the high surface to volume ratio of clay platelets, three parameters are important 1) have a higher degree of exfoliation of clay sheets into polymer matrix 2) achieve the highest degree of dispersion of clays into the matrix 3) achieve strong interfacial interactions between clay platelets and PU matrix [15,20,21].

Cloisite C30B platelets are held together by weak Vander Waals forces or hydrogen bonding. The clay platelets can be held apart either by chemical methods or by mechanical/physical methods [22]. Chemical methods of producing

exfoliations are *in situ* polymerization etc. whereas mechanical methods of producing exfoliation are grinding, high energy ball mill, and ultrasonication, although the degree and nature of exfoliation of clay dispersion are not always well defined. A few of the researchers have tried to explain the degree of exfoliation and dispersion [23,24]. Different processing techniques are having different advantages like sonication, enhance the exfoliation process, provide higher clay surface area, and more stable exfoliation [19,22-26]. High-speed stirring, high shear mixer, grinding, melt processing, as well as extrusion, are not able to generate the surface area of clays and unable to exfoliate the clay platelets neither can expand the interlayer gallery spacing for the platelets to lose their structural identity [11,17,19,24,27]. The high rotating speed of the instruments generates a higher enough processing temperature, due to the high shear forces exerted by the instruments, to degrade or to decompose the organically modifies clays [28]. This effectively alters the interface between organically modified clays and polymer. This study may help in the selection of processing instruments, their operational time as well as their



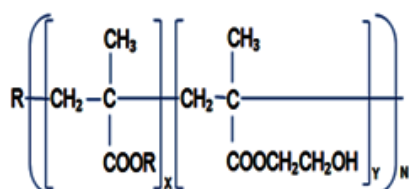
operational sequencing to achieve a high degree of exfoliation and dispersion of clays in the PU matrix.

In this study, we have tried to explore the different techniques of the combination of ultrasonic bath (USB) and probe sonicator (PS) i.e. parallel and series, for processing clays into the polymer matrix and to visualize their impact on the mechanical properties of the coatings. We have replaced PS with mechanical homogenizing mixer M (M@40rpm) to visualize the impact on the properties of the coatings. Mechanical properties of the coatings differentiate with the processing techniques and are characterized by nano-indentation.

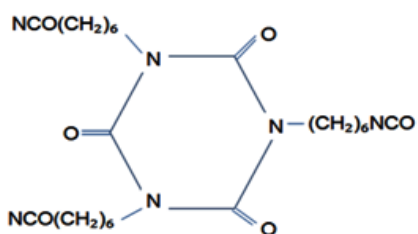
## Materials Used

Acrylic polyol (Macryl-60140 with a molecular weight of 10000, %NMV  $60 \pm 2$  @  $120^\circ\text{C}$ , hydroxyl value is 140mg KOH/Kg) was supplied by Macro Polymers Private Ltd. Ahmadabad, hexamethylene diisocyanate trimer, supplied by Wallmaax Paints Private Ltd. Kochi(Kerala). Cloisite C30B by Southern Clay Products, USA. Solvent n-butyl acetate was supplied by Loba Chemie Pvt. Ltd. Mumbai (India). The chemical

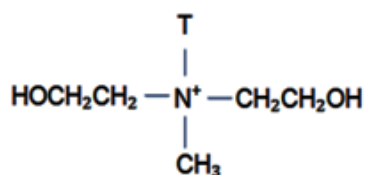
structure of Cloisite C30B, acrylic polyols, diisocyanates (Figure 1).



(a) Acrylic Polyol



(b) Hexamethylene Diisocyanate Trimer



(c) Cloisite C30B

Figure 1. Chemical structures of materials used (a) Acrylic polyol (b) Hexamethylene diisocyanate trimer (c) Cloisite C30B

## Experimentation

PU coatings were prepared according to the ASTM standard D823-95, before preparing the coatings cloisite (0.3gms, 1%wt./wt. of the total formulation) was sonicated in the solvent n-butyl acetate for 2hours in the ultrasonic bath. The polyol is added and sonicated in USB for 24hours and then processed under parallel and series sequence of USB and PS before curing with the diisocyanate. Probe sonicator, Hielscher, 230volts, @30kHz, and an ultrasonic bath are used in parallel combination and series combination for dispersion of clay platelets. The dispersed emulsion is cured by diisocyanate and mixed by a mixer for the preparation of coatings. The plan of work is shown in Figure 2.

Coatings were prepared on 10mmx10mmx1mm mild steel panels. The coatings were cured at room temperature  $25\pm 2$  °C for seven days as per ASTM D1640-03 standards and then characterized. Before the preparation of coatings, MS panels were treated and cleaned according to the ASTM standard D609-00. Free films were peeled out from HDPE sheets for characterization

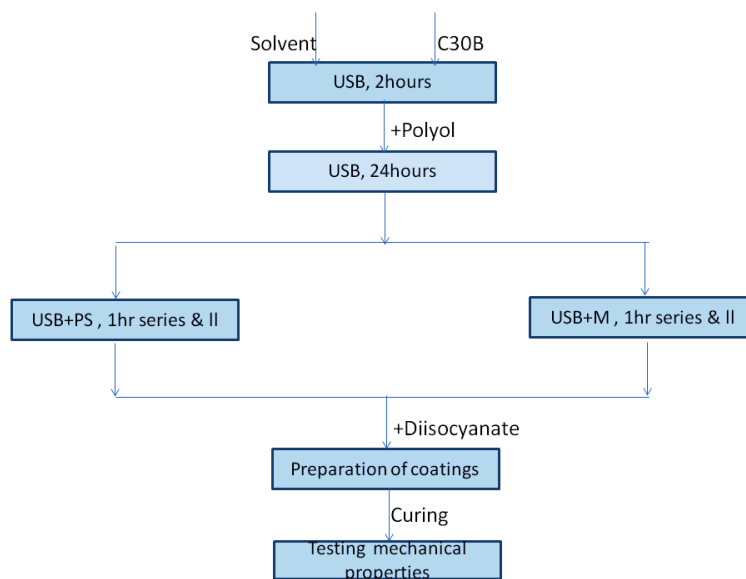


Figure 2. Plan of work

and analysis. The nomenclature of the samples is given in Table 1.

Table 1. Nomenclature and labeling of the samples

Sample	Description
PU	Polyurethane Reference sample
C30B-PS-	Polyurethane+C30B, Parallel sequencing of USB and PS
C30B-PS-	Polyurethane+30B, Series sequencing of USB and PS
C30B-M-P	Polyurethane+C30B, Parallel sequencing of USB and M
C30B-M-S	Polyurethane+C30B, series sequencing of USB and M

## Characterization

### Mechanical Properties by nanoindentation

Hysitron TI 950 TRIVO nano indenter was used for nanoindentation studies, with Berkovich Pyramidal diamond indenter of 100nm diameter. The maximum load applied was 1000 $\mu$ N with an increment of 200 $\mu$ N per second and the holding time at maximum load was 2 seconds. 1cmx1cm coated MS panels were used for this study. Each loading was done at atleast five different points in the sample and an average of these readings is reported. The maximum indentation depth at the maximum load applied is  $h_{max}$ . Residual depth is  $h_r$ , and  $h_o$  is the depth of indentation which can be recovered after releasing the load. Figure 3, image (b) [29] is the side view of the indentation before load and after releasing the load. Stiffness can be calculated from the slope of the unloading curve at maximum load i.e.  $dP/dh$  [20,29,30]. The hardness value is (H) resistance of a material against local surface deformation, is

$$H = \frac{P_{max}}{A} \quad (1)$$

Where  $A$  is the projected area between the sample and indenter.  $A = 24.5h_c^2$  [4,30,31] (Figure 3, image (a)). Reduced modulus can be calculated using Equation (2).

$$Er = \frac{1}{\beta} \times \frac{\sqrt{\pi}}{2} \times \frac{S_{max}}{\sqrt{A}} \quad (2)$$

Where  $S_{max}$  is the slope of unloading curve at the point of maximum loads,  $\beta$  is a constant and is a correction factor for indenter ( $\beta \sim 1.07$ ) depends upon the geometry of the indenter [23,29,31], and elastic modulus can be calculated from the reduced modulus by Equation (3) and Equation (4)

$$\frac{1}{Er} = \frac{1-\nu^2}{E} + \frac{1-\nu_i^2}{E_i} \quad (3)$$

$$E = E_i \times$$

$$\frac{Er(1-\nu^2)}{\{E_i - Er(1-\nu_i^2)\}} \quad (4)$$

Where  $E$  is the elastic modulus of coating,  $\nu$  is Poisson's ratio of coating,  $E_r$  is reduced modulus of coating,  $E_i$  is the elastic modulus of indenter and  $\nu_i$  is Poisson's ratio of the indenter. For diamond indenter  $E_i = 1141$  GPa,  $\nu_i = 0.07$  and  $\nu = 0.3$  due to polymer matrix dominated response [21,31].

Plastic deformation(%) was also calculated by Equation (5) as residual indentation

depth divided by maximum indentation depth [31,32].

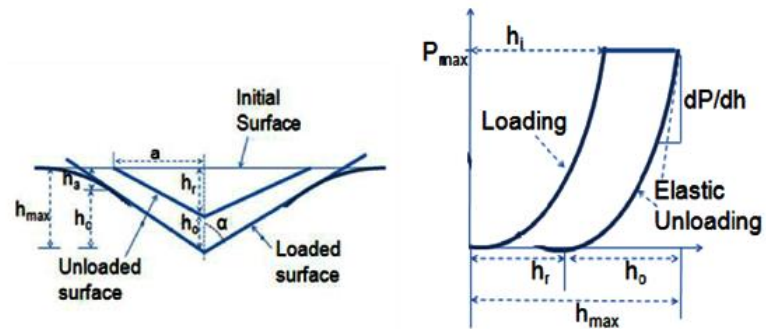


Figure 3. Standard figures of nanoindentation (a) View of the coating after nanoindentation (b) Load vs indentation depth

$$Plastic\ deformation(\%) = \frac{h_r}{h_{max}} \times 100 \quad (5)$$

Percent elasticity is calculated by Equation (6) and is recovered indentation depth after releasing the load ( $h_o$ ) divided by maximum indentation depth ( $h_{max}$ ).

$$Elasticity(\%) = \frac{h_o}{h_{max}} \times 100 \quad (6)$$

Creep is the strain rate of deformation at constant load and is calculated by Equation (7) [33].

$$Creep = \frac{\Delta\gamma}{\Delta t} \quad (7)$$

Where  $\Delta\gamma = (h_{max} - h_i) \div h_i$  and  $\Delta t$  is constant load time and is 2seconds.

## Results & Discussions

Nanoindentation is having high precision to determine the mechanical properties of the coatings. Loading and unloading curves are plotted against the indentation depth at varying loads and the loading-unloading cycles were completed. Mechanical properties were calculated from loading-unloading curves as discussed earlier by Oliver Pharr equations and are listed in Table 2.

Comparing curves of PU and PU/C30B coatings, if the shift of the peak is towards the left means the maximum indentation depth is lesser and the slope of the loading-unloading curve is increasing, due to the increased hardness of the coatings. The detailed load vs indentation depth of PU and PU/clay composites are given in Figure 4. The maximum indentation depth in PU is 1171nm, 1280 nm for C30B-PS-P and 1256nm for C30B-PS-S, the resistance to penetration is more in C30B-PS-S, having a high hardness as compared with



C30B-PS-P whereas pure PU has a maximum hardness. There is a minor increase in the hardness is 1.4% in the case of C30B-PS-S than C30B-PS-P but the hardness is achieving lower digits than the pure PU. This may be due to the flexibility of cloisite C30B towards nanoindentation or the weak hydrogen bonding of cloisite C30B with the hardener of PU as compared with strong intramolecular covalent bonding/ionic interactions of PU. The increase in the elastic modulus is 6% in C30B-PS-P as compared with C30B-PS-S. Hardness is inversely proportional to the area of indentation as given in equation (1) whereas modulus and stiffness are directly proportional to the slope of the unloading curve  $dP/dh$ . Stiffness is 2.9% higher in C30B-PS-P and 6.6% in C30B-PS-S as compared with pristine PU. This may be due to the high degree of exfoliation achieved in parallel sequencing of PS and USB and makes the object stiffer which is also a cause for higher modulus.

The residual depth is 803nm in PU, 975nm in C30B-PS-P, and 922nm in C30B-PS-S i.e. Plastic deformation is maximum in C30B-PS-P and minimum in PU. The addition of C30B increases the plasticity of PU i.e. higher the exfoliation higher the plasticity i.e. unrecoverable indentation. Plastic

deformation is higher at 11% and 3.7% in C30B-PS-P than PU and C30B-PS-S, indicates that the unrecoverable deformation is higher in parallel sequencing. Elastic deformation is the ratio of recovered depth to the maximum depth. The recovered elastic deformation indicates that the sample has recovered the indentation depth and the left residual depth is unrecoverable or permanent.

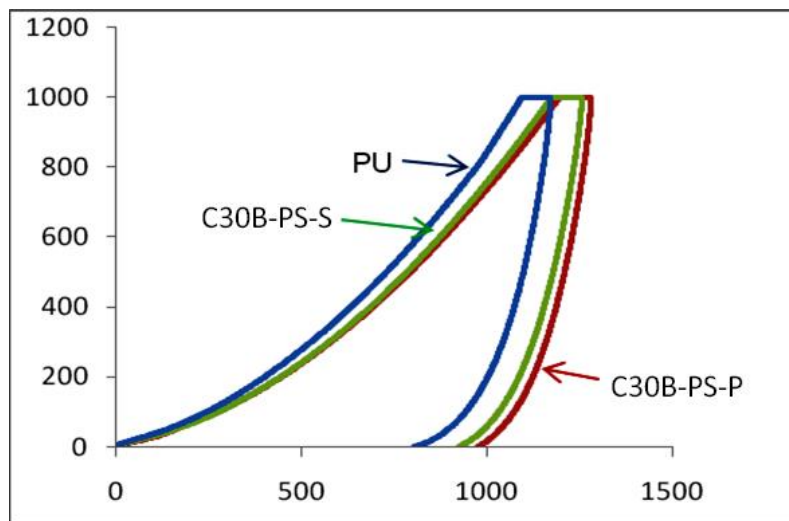


Figure 4. Loading unloading curves of PU, C30B-PS-P, and C30B-PS-S

The constant load curve is used to calculate the creep. Creep is strain rate of deformation  $\Delta\gamma/\Delta t$ -time rate of strain,  $\Delta\gamma = (h_{\max} - h_i)/h_i$  Constant load

Table 2 Mechanical properties of PU, C30B-PS-P, and C30B-PS-S

Sample	PU pure	C30B-PS-P	C30B-PS-S
Stiffness ( $\mu\text{N/nM}$ )	7.18	7.39	6.93
Modulus Reduced (GPa)	2.68	2.48	2.34
Elastic Modulus (GPa)	2.44	2.26	2.13
Hardness (GPa)	0.178	0.144	0.146
Plastic Deformation (%)	68.57	76.12	73.4
Elastic Deformation (%)	31.43	23.88	26.6
Creep (1/s)	.035	.036	.035

time 2sec where  $h_i$  can be measured as indentation depth of loading curve at maximum load [29]. The creeps depth is the depth of indentation at constant load and creep depth is maximum length minus initial indentation depth i.e. 77nm, 86nm, and 82nm in PU, C30B-PS-P, and C30B-PS-S, is also higher in parallel sequencing, C30B favors the creep.

The mechanical properties like stiffness, elastic modulus, and creep show higher swing in composite coatings C30B-PS-P, whereas hardness is higher in C30B-PS-S, possibly due to two main reasons. One is that there is lesser exfoliation of clay platelets in C30B-PS-S (series sequencing of

processing) and 2<sup>nd</sup> is the weak hydrogen bonding between C30B and the hardener of PU [24, 27].

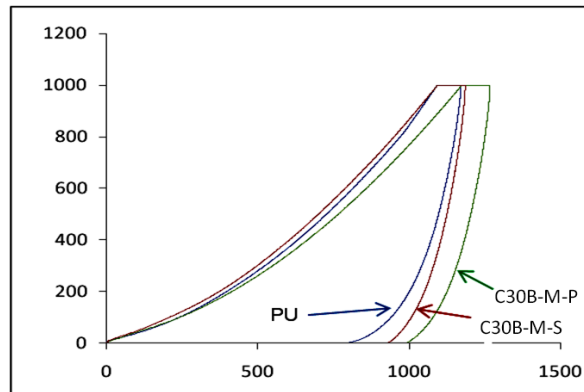


Figure 5. Loading unloading curves of PU, C30B-M-P, and C30B-M-S

In another study, we replaced the probe sonicator (PS) with the mechanical homogenizing mixer (M) and used ultra sonicator bath (USB) and (M) in parallel and series for processing the C30B into polyol. After swelling the nanofiller for 2hours in n-butyl acetate using USB, and exfoliated in polyol for 24hours using USB before processing in parallel and series combination of USB and M. Coatings were prepared by natural pouring, to cure the processed samples with hardener and mechanical properties were evaluated by nanoindentation (Table 3, Figure 5). Mechanical properties show a higher swing in composite

coatings as compared with pristine PU, as there is effective exfoliation-dispersion due to USB and a good length of time for processing [24,27]. The increase in the modulus 16%, in stiffness is 21.5%, in creep 2%, and a decrease in hardness is 10% in C30B-M-S as compared with PU.

Table 3. mechanical properties of PU, C30B-M-P and C30-M-S

Sample	PU	C30B-M-P	C30B-M-S
Stiffness ( $\mu\text{N/nM}$ )	7.18	8.41	8.72
Elastic Modulus (GPa)	2.44	2.5	2.83
Modulus Reduced (GPA)	2.68	2.74	3.09
Hardness (GPa)	0.178	0.136	0.16
Plastic Deformation (%)	68.57	78.45	78.7
Elastic Deformation (%)	31.43	21.55	21.3
Creep (1/s)	.035	.039	.042

## Conclusions

Mechanical properties show the highest swing in the series sequencing of USB and M as compared with all other setups. Moreover, USB and M give overall higher mechanical properties as compared with USB and PS. This may be because the nanocomposites processed through USB and M gives higher exfoliation and dispersion of clay platelets into the polymer matrix as compared with the nanocomposites processed through USB and

PS. This is due to the design and nature of processing instruments, as USB helps to exfoliate the platelets whereas M disperse the exfoliated clay platelets effectively as compared with USB and PS, both are sonicators which helps to exfoliate the clay platelets but may hinder in dispersing the exfoliated clays. Moreover, series sequencing of USB and M is more effective in exfoliating and dispersing the clay platelets than parallel sequencing because dispersion is effective only when exfoliation is complete.

The parallel sequencing of USB and PS gives higher properties and hence a higher degree of exfoliation/dispersion of clay platelets into the polymer matrix as compared with series sequencing. This depicts that the effective exfoliation of clay platelets and higher mechanical properties can be achieved while using the processing instruments or USB and PS simultaneously as compared with the series sequence. This may be because both the sonicators are effective in exfoliating the clay platelets and they are more effective when using simultaneously as compared with individual ones. In further studies, one should choose processing instruments that are effective in exfoliating the clay

platelets as well as are more effective in dispersing the same ones.

### Acknowledgment

I am thankful to Dr. Shanti Swaroop Bhatnagar University Institute of Chemical Engineering & Technology, Panjab University, Chandigarh for providing me the laboratory for conducting my research work, and again thanks for providing me necessary guidance and help. I pay my sincere thanks to Dr. Sanchita Chauhan and Dr. Gaurav Verma for their co-operation and guidance in conducting my research work. I also thanks Mr. Girish Sharma, Technical Director, Wallmaax Paints Pvt. Ltd., Kochi, Kerala, for supplying me with the necessary materials and guiding me for the research work.

### Declaration of conflicts of interest

The author(s) declared no potential conflicts of interest concerning the research, authorship, and/or publication of this article.

## References

### Journal Articles

1. K. P. Chandrashekhar, D. J. Harishchandra, S. P. Jayasinh, L. C. Bhushan, V. V. Gite, Functional antimicrobial and anticorrosive polyurethane composite coatings from algae oil and silver doped eggshell hydroxyapatite for sustainable development, *Progress in Organic Coatings*, 126 (2019), 127-136
2. B. Adak, B. S. Butola, M. Joshi, Effect of organoclay-type and clay-polyurethane interaction chemistry for tuning the morphology, gas barrier and mechanical properties of clay/polyurethane nanocomposites, *Applied Clay Science*, 161 (2018), 343-353
3. L. Zaidi, K. Mustapha, S. Bruzard, A. Bourmaud, Y. Grohens, Effect of natural weather on the structure and properties of poly(lactide)/Cloisite 30B nanocomposites, *Polymer Degradation and Stability*, 95 (2010), 1751-1758
4. C. Saha, C. K. Tapan, K. N. Singha,



- Synthesis and Characterization of elastomeric Polyurethane and PU/Clay Nanocomposites Based on an Aliphatic Diisocyanate, *Journal of applied polymer science*, 130 (2013), 3328-3334
5. S. Cakie, C. Lacnjevac, J. Stamenkovic, N. Ristic, L. Takic, M. Barac and M. Gligoric, Effects of the acrylic polyol structure and the selectivity of the employed catalyst on the Performance of two-component aqueous polyurethane coatings, *Sensors*, 7 (2007), 308-318
  6. Satriananda, R. Medyan, M. Sri and M. Farid, Polyurethane/clay nanocomposites from palm oil for surface-coating applications, *Polymers from Renewable Resources*, 9 (2018), 103-110
  7. D. Guilherme, P. Manoela, L. Rosane, P. Mathilde, L. R. Christophe, M. Pierre, M. François and E. Sandra, Hybrid Pu/Synthetic Talc/Organic Clay Ternary Nanocomposites: Thermal, Mechanical and Morphological Properties, *Polymers and Polymer Composites*, 26 (2018), 127-140
  8. J. H. Li, R. Y. Hong, M. Y. Li, H. Z. Li, Y.

- Zheng, J. Ding, Effects of ZnO nanoparticles on the mechanical and antibacterial properties of polyurethane coatings, *Progress in Organic Coatings*, 64 (2009), 504–509
9. P. A. Charpentier, K. Burgess, L. Wang, R. R. Chowdhury, A.F. Lotus and G. Moula, Nano- TiO<sub>2</sub>/polyurethane composites for antibacterial and self-cleaning coatings, *Nanotechnology*, 23 (2012), 425606
  10. C. Y. Chee, S. Nurehan, Effect of nano-silica filled polyurethane composite coating on polypropylene substrate, *Journal of Nanomaterials*, 2013 (2013), 1-8
  11. M. Mirzataheri, S. Khamisabadi, S. Ali, Characterization of styrene-co-butyl acrylate/cloisite Na+nanocomposite film synthesized via soap free emulsion polymerization, *Progress in Organic Coatings*, 99 (2016), 274–281
  12. G. Verma, A. Kaushik, A. K. Ghosh, Preparation, characterization and properties of organoclay reinforced polyurethane nanocomposite coatings,

- Journal of Plastic Film & Sheeting, 29 (2012), 56–77
13. G. Verma, A. Kaushik, A. K. Ghosh, Comparative assessment of nanomorphology and properties of spray coated clear polyurethane coatings reinforced with different organoclays, Progress in Organic Coatings, 76(2013), 1046–1056
  14. L. Thair, I. K. Jassim, R. K. Sanaa, J. F. Hammody, H. K. Mohammed, Corrosion protection of carbon steel oil pipelines by unsaturated polyester/clay composite coating, American Scientific Research Journal for Engineering, Technology, and Sciences (ASRJETS), 18 (2016), 108-119
  15. R. T. Fox, H. Zhang, M. A. Barger, C. Han, M. Paquette, Natural and synthetic clay-filled coatings for insulation barrier applications, Journal of Coatings Technology and Research, 13 (2016), 181–189
  16. O. Kamigaito, What can be improved by nanometer composites?, Journal Jpn Soc Powder Powder Metal, 38 (1991),

315–321

17. H. U. Zaman, M. D. H. Beg, Effect of Processing Parameters on the Properties of Rigid PVC/Organoclay Nanocomposites, *J. of Poly. Mat.*, 31 (2014), 77-88
18. R. Pablo, E. Germán, S. Guillermo, Q. Javier, Micro and nanocomposites of polybutadiene based polyurethane liners with mineral fillers and nanoclay: thermal and mechanical properties, *Open Chemistry*, 15 (2017), 46-52
19. M. Jose, H. Alonso, M. Eva, J. C. Little, S. S. Cox, Transport properties in polyurethane/clay nanocomposites as barrier materials: Effect of processing conditions, *Journal of Membrane Science*, 337 (2009), 208–214
20. X. Jingshui, C. Lihua, Z. Zhong, Z. Ling, X. Cen, H. Weishan, X. Yashui and Y. Liping, Highly exfoliated montmorillonite clay reinforced thermoplastic polyurethane elastomer: in situ preparation and efficient strengthening, *RSC Advances*, 9 (2019), 8184- 8196
21. M. Boumaza, R. Khan, S. Zahrani, An

- experimental investigation of the effects of nanoparticles on the mechanical properties of epoxy coating, *Thin Solid Films*, 620 (2016), 160-164
22. T. T. Zhu, C. H. Zhou, F. B. Kabwe, Q. Q. Wu, C. S. Li, J. R. Zhang, Exfoliation of montmorillonite and related properties of clay/polymer nanocomposites, *Applied Clay Science*, 169 (2019), 48-66
23. X. Hesheng, J. S. Stephen and M. Song, Relationship between mechanical properties and exfoliation degree of clay in polyurethane nanocomposites, *Polymer International*, 54 (2005), 1392-1400
24. X. Hesheng and M. Song, Intercalation and exfoliation behavior of clay layers in branched polyol and polyurethane/clay nanocomposites, *Polymer International*, 55 (2006), 229-235
25. G. Choudalakis, A. G. Gotsis, Morphology and gas transport properties of acrylic resin/Bentonite nanocomposite coatings, *Progress in Organic Coatings*, 77 (2014), 845–852
26. Rhoney, S. Brown, N. E. Hudson, R. A.

- Pethrick, Influence of processing method on the exfoliation process for organically modified clay systems. I. Polyurethanes, *Journal of Applied Polymer Science*, 91 (2004), 1335-1343
27. T. P. Mohan, D. Kay and K. Kanny, Barrier and biodegradable properties of corn starch- derived biopolymer film filled with nanoclay fillers, *Journal of Plastic Film & Sheeting*, 33 (2017), 309-336
28. M. Tomica, B. Dunjica, M. S. Nikolica, J. Maletaskicb, V. B. Pavlovicc, J. Bajata, J. Djonlagic, Dispersion efficiency of montmorillonites in epoxy nanocomposites using solution intercalation and direct mixing methods, *Applied Clay Science*, 154 (2018), 52-63
29. J. Nemecek, *Nanoindentation Basics, theory, principles and techniques*. Czech Technical University in Prague, Department of Mechanics, Thakurova 7. 166, 29 Praha 6, Czech Republic, 2015
30. H. Mohammad, S. Chowdhury, Y. Song, P. Y. Zeng, C. J. Grunlan, A.A. Polycarpou, Nanomechanical behavior of high gas barrier multilayer thin films, *ACS*

- Applied Materials and Interfaces, 8 (2016), 11128–11138
31. H. Ghermezcheshme, M. Mohseni, H. Yahyaei, Use of nanoindentation and nanoscratch experiments to reveal the mechanical behavior of POSS containing polyurethane nanocomposite coatings: The role of functionality, Tribology International, 88 (2015), 66–75
  32. Y. Wang, L. Zhang, Y. Hu, L. Chunzhong, Comparative study on optical properties and scratch resistance of nanocomposite coatings incorporated with flame spray pyrolyzed silica modified via in-situ route and ex-situ route, Journal of Materials Science & Technology, 32 (2016), 251–258
  33. S. J. Nikkhah, H. Hojati & M. R. Moghbeli, Self-Cross-linking acrylate copolymer/ organoclay nanocomposite emulsion coating: Nanoindentation and nanoscratch behavior, Polymer-Plastics Technology and Engineering, 53 (2014), 268–277

## Biography

Balwinder Singh has completed his Ph.D. from the department of Dr. Shanti Swaroop Bhatnagar University Institute of Chemical Engineering & Technology, Panjab University, Chandigarh, in the area of Nanotechnology and Polymers/Coatings. Mr. Balwinder received his BE and ME in Chemical Engineering from the same department and is having around 20 years industrial experience. He has worked with the pharmaceutical giants like Nectar Lifesciences Ltd. Derabassi, Inswift labs ltd. Derabassi, and chemical Industries like Modi Alkalies & Chemicals ltd. Alwar (Rajasthan) etc. His research areas are in nanotechnology, materials, polymer composites and coatings.